The Astrophysical Journal Letters, 831:L13 (7pp), 2016 November 10 doi:10.3847/2041-8205/831/2/L13

PLASMA HEATING INSIDE INTERPLANETARY CORONAL MASS EJECTIONS BY ALFVÉNIC FLUCTUATIONS DISSIPATION

Hui Li[1], Chi Wang[1], Jiansen He[2], Lingqian Zhang [1], John D. Richardson[3], John W. Belcher[3], and Cui Tu[4]
[1] State Key Laboratory of Space Weather, National Space Science Center, CAS, Beijing, 100190, China; hli@spaceweather.ac.cn
[2] School of Earth and Space Sciences, Peking University, Beijing, 100871, China
[3] Kavli Institute for Astrophysics and Space Research, Massachusetts Institute of Technology, Cambridge, MA, USA
[4] Laboratory of Near Space Environment, National Space Science Center, CAS, Beijing, 100190, China
Received 2016 August 16; revised 2016 October 19; accepted 2016 October 20; published 2016 November 3

ABSTRACT

Nonlinear cascade of low-frequency Alfvénic fluctuations (AFs) is regarded as one of the candidate energy sources that heat plasma during the non-adiabatic expansion of interplanetary coronal mass ejections (ICMEs). However, AFs inside ICMEs were seldom reported in the literature. In this study, we investigate AFs inside ICMEs using observations from *Voyager* 2 between 1 and 6 au. It has been found that AFs with a high degree of Alfvénicity frequently occurred inside ICMEs for almost all of the identified ICMEs (30 out of 33 ICMEs) and for 12.6% of the ICME time interval. As ICMEs expand and move outward, the percentage of AF duration decays linearly in general. The occurrence rate of AFs inside ICMEs is much less than that in ambient solar wind, especially within 4.75 au. AFs inside ICMEs are more frequently presented in the center and at the boundaries of ICMEs. In addition, the proton temperature inside ICME has a similar "W"-shaped distribution. These findings suggest significant contribution of AFs on local plasma heating inside ICMEs.

Key words: acceleration of particles – solar wind – Sun: coronal mass ejections (CMEs) – turbulence – waves

1. INTRODUCTION

Coronal mass ejections (CMEs) are spectacular large-scale disturbed structures involving great explosion of solar material into the heliosphere (e.g., Gopalswamy 2010). Solar wind structures or interplanetary manifestations of CMEs are now generally referred to as interplanetary coronal mass ejections (ICMEs), which are the heliospheric counterparts of CMEs at the Sun (e.g., Gosling 1990; Neugebauer & Goldstein 1997).

ICMEs often expand in size with radial distance in the inner heliosphere since their internal pressures are generally higher than the ambient solar wind, and their leading edges usually move faster than the trailing edges (see Burlaga 1995 and references therein). The radial width increases with distance out to ~15 au (Wang & Richardson 2004; Liu et al. 2005); beyond this distance, the widths are relatively constant because ICMEs reach equilibrium with the background solar wind (Wang et al. 2005; Liu et al. 2006; Richardson et al. 2006).

For an expanding ICME, the proton temperature would be expected to decrease more quickly within the ICME than in the ambient solar wind due to adiabatic cooling. However, the proton temperature inside ICMEs does not behave even qualitatively as expected. Liu et al. (2005) and Wang et al. (2005) found that the proton temperature inside the ICMEs from 0.3 to 5.4 au decreases slower than in the background solar wind. Wang & Richardson (2004), Richardson et al. (2006), and Liu et al. (2006) combined *Voyager* 1 and *Voyager* 2 data and extended such findings out to 30 au. The polytropic index γ was determined empirically to be $1.15 \sim 1.33$, implying considerable local plasma heating within ICMEs.

The most probable energy source of plasma heating within ICMEs is believed to come from the magnetic field. However, the mechanism that dissipates magnetic energy into thermal energy is still an open question. In the literature, several candidate mechanisms were proposed to heat the CME plasma, which are listed as follows: (1) outflows from the CME current sheets (Bemporad et al. 2007); (2) kink instability (e.g., Rust & LaBonte 2005); (3) small-scale magnetic reconnection (Furth et al. 1963); (4) damping of MHD waves; (5) thermal conduction along the magnetic field (Landi et al. 2010); (6) energetic particles; (7) counteracting flows (Filippov & Koutchmy 2002); and (8) ohmic heating from net current in the flux rope (Murphy et al. 2011).

Nonlinear cascade of low-frequency Alfvénic fluctuations (AFs), which transfers energy from large scales down to small kinetic scales for further dissipation, is generally regarded as one candidate energy source for the heating of ICME plasma. It can preferentially heat heavy ions within ICMEs as observed (Tu & Marsch 1995; Tam & Chang 1999; Kasper et al. 2008; Wang et al. 2014). Galinsky & Shevchenko (2012) showed that heavy ions could be heated due to interactions between anti-sunward and sunward AFs. Liu et al. (2006) found turbulence inside an ICME at 3.25 au and suggested that magnetic turbulence dissipation seems sufficient to explain the ICME heating; they assumed that the turbulence was driven by AFs, though AFs were seldom reported inside 280 ICMEs from 0.3 to 20 au. To our knowledge, quite limited numbers of AF events have been published in the literature. Marsch et al. (2009) found possible AFs lasting for almost one hour in an ICME detected at 0.7 au. Yao et al. (2010) later presented clear AFs with a 2 hr duration inside an ICME observed at 0.3 au.

Traditional diagnosis of AFs may underestimate the degree of Alfvénicity, and thus possibly miss some AFs. Li et al. (2016a) proposed a new approach to search for AFs, which could reduce the uncertainties in identifying AFs. In this study, we apply this AF diagnosis approach to identify AFs inside ICMEs from 1 to 6 au based on *Voyager* 2 data. Abundant AFs are found within ICMEs. Clear indirect evidence of the contributions of AFs on ICME plasma heating is provided.

2. DIAGNOSIS OF AFs WITHIN ICMEs

The differences of ICMEs lie in the different signatures of magnetic field, plasma, composition, and energetic particle.

However, the identification of ICMEs still remains a subjective undertaking. No single characteristic has proved both necessary and sufficient to define the presence of ICMEs. The currently used signatures for the in situ identification of ICMEs at 1 au have been well summarized (see Zurbuchen & Richardson 2006 and references therein). However, in the outer heliosphere, ICME identification becomes even more difficult. On one hand, some signatures of ICMEs are blurred through interaction with the ambient solar wind. On the other hand, current available measurements from the limited instruments cannot supply the complete set of variables required for comprehensive identification.

Wang & Richardson (2004) identified 147 probable ICMEs from hourly averaged solar wind plasma and magnetic field data by *Voyager* 2 between 1 and 30 au. The primary criterion they used is the abnormally low solar wind proton temperature proposed by Richardson & Cane (1995). This criterion compares the observed proton temperature T_p with the "expected" temperature $T_{\rm ex}$ appropriate for "normally expanding" with the observed solar wind speed V. $T_{\rm ex}$ (in units of 10^3 K) is calculated from the relationship derived by Lopez (1987):

$$T_{\rm ex} = \begin{cases} (0.031V - 5.1)^2/R^{0.6} & < 500\ {\rm km\ s^{-1}} \\ (0.51V - 142)/R^{0.6} & \geqslant 500\ {\rm km\ s^{-1}}. \end{cases} \quad (1)$$

They also examined the magnetic field and plasma parameters to exclude regions that may not be ICMEs, such as regions associated with heliospheric current sheet crossings. The determination of ICME boundaries is uncertain since different signatures usually have different boundaries. The boundaries chosen by them were generally coincident with the regions where $T_p/T_{\rm exp} = 0.5$ with some adjustments based on reduced magnetic field fluctuations.

In this work, we identify ICMEs mainly based on the probable ICME list of *Voyager* 2 given by Wang & Richardson (2004). In order to ensure the availability of combined magnetic field and plasma data with a temporal resolution of 48 or 96 s (which is adequate for analyzing AFs suggested by Li et al. 2016b) and to avoid the complications caused by the heating of interstellar pickup ions (Richardson & Smith 2003), we only use *Voyager* 2 data from 1977 December 1 to the end of 1979. During this time period, a total of 33 probable ICMEs were identified. Note that some minor adjustments of ICME boundaries have been done based on the data sets with a higher time resolution compared to hourly data sets used by Wang & Richardson (2004).

To reduce the uncertainties of AF diagnoses introduced in the determinations of the background magnetic field and the deHoffmann-Teller (HT) frame, we apply the approach proposed by Li et al. (2016a) to identify AFs within ICMEs. Instead of the original data sets, the bandpass-filtered signals of the plasma velocity and magnetic field observations are used to check the Walén relation as follows:

$$\delta \boldsymbol{V}_i = \pm \delta \boldsymbol{V}_{\rm Ai}. \quad (2)$$

Here, $\delta \boldsymbol{V}_i$ and $\delta \boldsymbol{V}_{\rm Ai}$ represent the bandpassed $\boldsymbol{V}$ (solar wind velocity) and $\boldsymbol{V}_{\rm A}$ (local Alfvén velocity) with the ith filter, respectively. The $-/+$ signs, respectively, denote the propagation parallel and anti-parallel to the background magnetic field. The parameter proposed by Li et al. (2016a, 2016b), E_{rr}, is used to assess the goodness of the degree of the Alfvénicity. Compared to previous parameters defined to represent the Alfvénicity, such as the Alfvén ratio, the Walén slope, the normalized cross helicity, the normalized residual energy, and the velocity–magnetic field correlation coefficient, E_{rr} is a more comprehensive and reliable quantity (Li et al. 2016b).

We apply a moving window with a width of 1 hr and a moving step of 5 minutes to calculate E_{rr} for each filtered data set. The AFs are defined as the intervals with $E_{rr} < 0.15$ as used by Li et al. (2016a). For 48 s *Voyager* 2 data, the filters are chosen to be 100–135 s, 135–180 s, 180–250 s, 250–330 s, 330–450 s, 450–600 s, 600–810 s, 810–1100 s, 1100–1480 s, and 1480–2000 s. For 96 s *Voyager* 2 data, the filters are chosen to be 200–250 s, 250–20 s, 320–400 s, 400–500 s, 500–630 s, 630–800 s, 800–1000 s, 1000–1260 s, 1260–1580 s, and 1580–2000 s.

3. AFs INSIDE AN ICME AT 4.73 au: A TYPICAL CASE

Figure 1 shows the overview of an ICME observed by *Voyager* 2 at ~4.73 au during 1979 February 17–23. The threshold value $T_p/T_{\rm ex} = 0.5$ is plotted as the horizontal dashed line in the fifth panel. As described previously, the primary criterion for identifying possible ICMEs, $T_p/T_{\rm ex}$, is well under 0.5 inside the ICME (hatched area). A monotonic declining of solar wind bulk speed and a cool proton thermal speed ($<20\ {\rm km\ s^{-1}}$) are other typical characteristics of a candidate ICME event observed beyond 1 au (Russell & Shinde 2003). For this event, the solar wind bulk speed decreases nearly monotonically across the ICME and the proton thermal speed within the ICME is less than $15\ {\rm km\ s^{-1}}$. The speed of the leading edge is $450\ {\rm km\ s^{-1}}$, which is faster than that of the trailing edge of $390\ {\rm km\ s^{-1}}$. The speed difference of $60\ {\rm km\ s^{-1}}$ suggests that the ICME is still expanding as it moves outward. This value is a little larger than the average expansion speed of an ICME at 4.73 au ($48 \pm 4\ {\rm km\ s^{-1}}$) estimated based on the empirical formula given by Liu et al. (2005). The density inside ICMEs beyond 1 au is often smaller than in the ambient solar wind. For this event, the density is generally $\leqslant 0.3\ {\rm cm^{-3}}$, less than the value in the ambient solar wind of $0.4\ {\rm cm^{-3}}$. In addition, the magnetic field strength has an enhancement during this event. These additional signatures give us more confidence that this event is an ICME event. The duration of this ICME is about 154.0 hr with an average solar wind speed of about $420\ {\rm km\ s^{-1}}$, which gives a radial width of about 1.55 au, which is a little larger than the average radial width of an ICME at 4.73 au (1.16 ± 0.04 au) estimated based on the empirical formula given by Liu et al. (2005). The time-frequency distribution of E_{rr} reveals that there exists many intervals of relatively pure AFs in the center and at both boundaries of the ICME, which are denoted by the green and blue regions.

Figure 2 shows two examples of AFs inside the ICME shown in Figure 1. The left panel shows the AFs during 0050–0250 UT on 1979 February 21. During this time interval, the solar wind is essentially incompressible with relative fluctuations $\delta N_p/N_p$ of 7.7% and $\delta|B|/|B|$ of 1.1%. However, the three components of $\boldsymbol{B}$ and $\boldsymbol{V}$ have large-amplitude fluctuations that have a strong positive correlation. The correlation coefficients for the R, T, and N components are 0.84, 0.89, and 0.88, respectively. Such a strong correlation and incompressibility indicate the presence of AFs propagating anti-parallel to the background magnetic field, which is assumed to be the mean magnetic field during this time interval (−0.79, 0.60, 0.22) nT. From the time-frequency

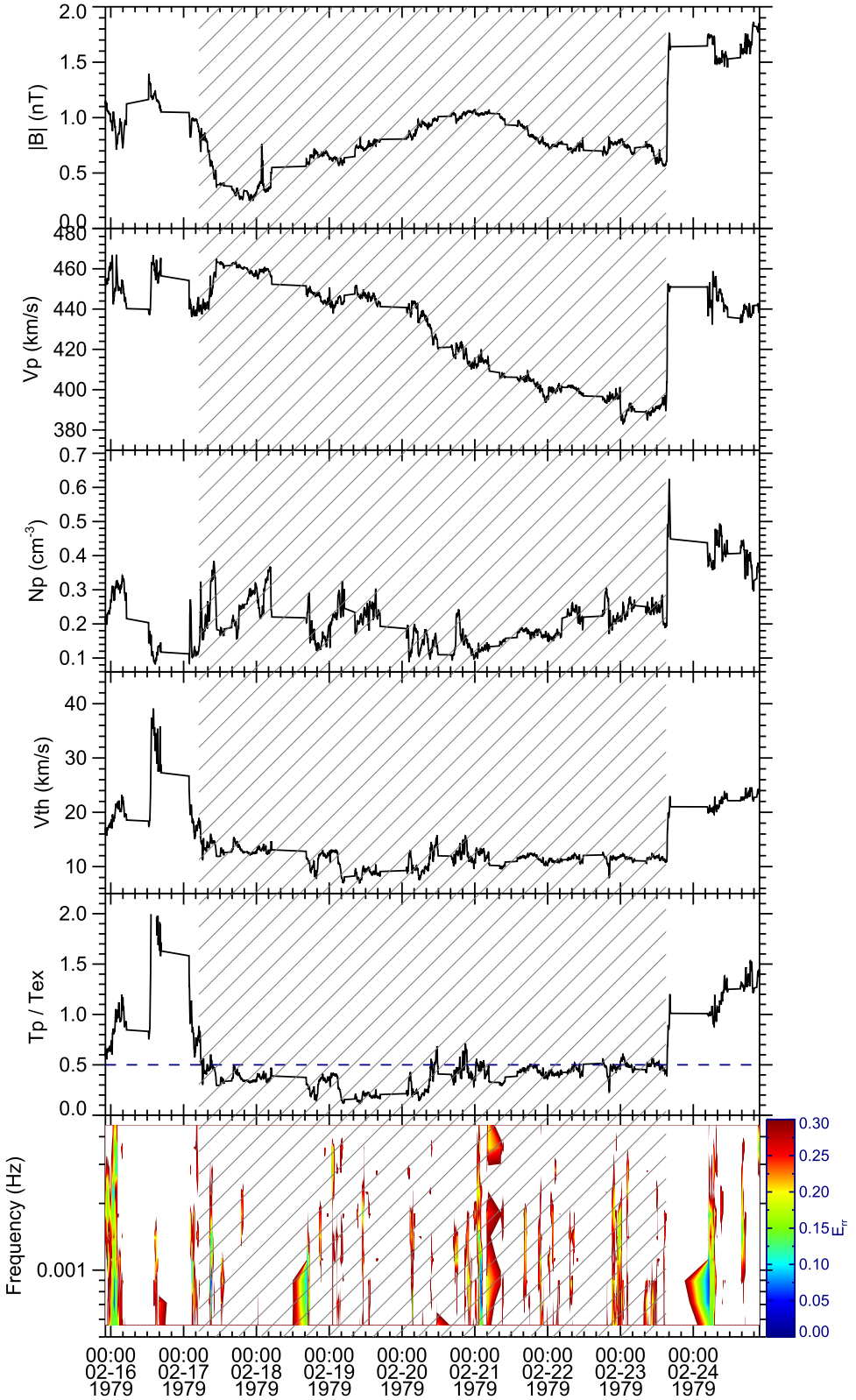

Figure 1. Overview of an ICME (hatched area) observed by *Voyager* 2 at ~4.73 au. From top to bottom, the panels show the magnetic field strength ($|B|$), the solar wind bulk speed (V_p), the proton number density (N_p), the proton thermal speed ($V_{\rm th}$), the ratio of the observed to the expected temperature ($T_p/T_{\rm ex}$), and E_{rr}, respectively.

distribution of E_{rr}, it is clear that the AFs during this interval are not periodic like a monochromatic wave, instead are broadband with different frequencies at different times. For example, the wave periods of relatively pure AF during 0050 and 0150 UT are generally 630–800 s, and the wave periods during 0135–0230 UT change to 800–2000 s. The right figure shows the AFs from 2100 UT on 1979 February 22 to 0040 UT on 1979 February 23. The relative fluctuations of $\delta N_p/N_p$ and

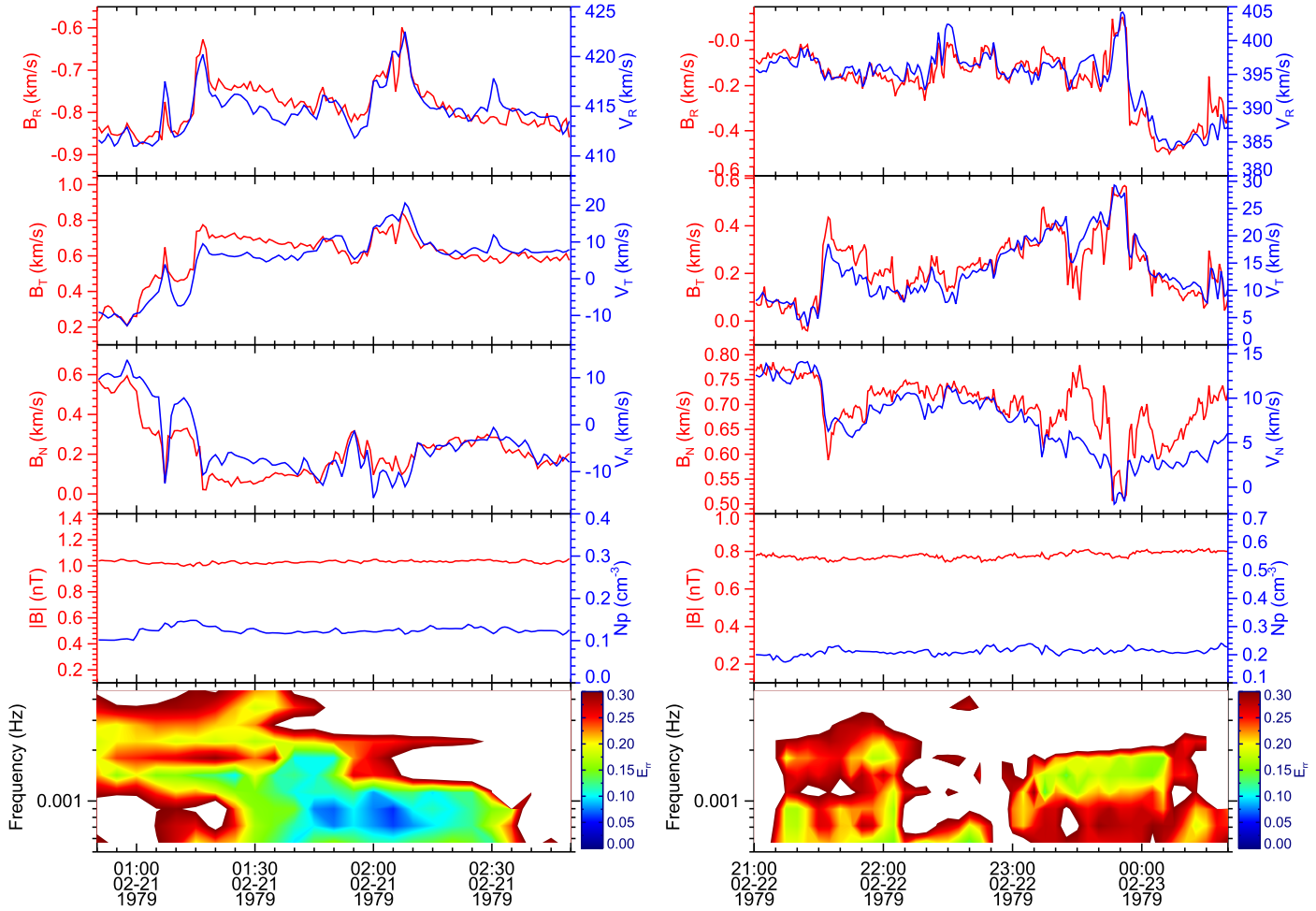

Figure 2. Two AFs inside the ICME shown in Figure 1. Left: 0050–0250 UT on 1979 February 21; right: 2100 UT on 1979 February 22 to 0040 UT on 1979 February 23. The first three panels show the magnetic field (***B***, in red) and solar wind velocity (***V***, in blue) in the RTN coordinates, and the fourth panels show the magnetic field strength (|*B*|, in red) and proton number density (N_p, in blue), and the bottom panels show E_{rr}.

$\delta|B|/|B|$ are insignificant, 5.6% and 2.2%, respectively. This indicates that the solar wind is incompressible. However, the fluctuations in the three components of ***B*** and ***V*** in the RTN coordinates have large amplitudes and a strong positive correlation. The correlation coefficients for the R, T, and N components are 0.93, 0.88, and 0.82, respectively. The background magnetic field, which is assumed to be the mean magnetic field during this time interval, is (−0.17, 0.22, 0.70) nT. Obviously, there exists relatively pure AFs during this time interval, which propagate anti-parallel to the N axis in the RTN coordinates. This is confirmed from the time-frequency distribution of E_{rr} as well. The wave periods of relatively pure AF during 2110 and 2210 UT are generally 1260–2000 s, and the wave periods during 2310–0010 UT change to 630–1000 s.

4. STATISTICAL CHARACTERISTICS OF AFs INSIDE ICMEs

The results shown in Section 3 suggest that relatively pure AFs can and do exist inside ICMEs. Figure 3 (left) shows the dependence of the percentage of AF duration inside ICMEs on heliocentric distance. Among 33 probable ICMEs observed by *Voyager* 2 from 1977 December 1 to the end of 1979, AFs could be identified inside 30 ICMEs, a percentage of 91%. Besides, it is obvious that the percentage of AF duration reduces generally linearly as ICMEs expand and move outward. The dashed line represents the linear fitting result with the correlation coefficient of −0.73. For ICMEs at ∼2 au, the percentage of AF is about 20%, while for ICMEs at ∼6 au, the percentage of AF decreases significantly to about 5%.

Figure 3 (right) shows the statistical characteristics of AF occurrence rate inside ICMEs and in ambient solar wind at different heliocentric distance. Note that the AF occurrence rates inside ICMEs were calculated from dividing the total duration of AFs within ICMEs into the total ICME duration, but not from the mean values of scattered dots in Figure 3 (left). The AF occurrence rate in ambient solar wind is obtained from a similar calculation methodology. In order to make the comparison of AF occurrence rates inside ICMEs and in ambient solar wind more reliable in terms of statistical significance, we divide the *Voyager* 2 observations into seven time intervals and make sure that the total time durations of AFs in each time interval are statistically sufficient. In general, both the AF occurrence rates inside ICMEs and in ambient solar wind decrease with heliocentric distance. However, the occurrence rate of AFs inside ICMEs is found to be less than that in ambient solar wind, especially with a heliocentric distance less than 4.75 au, which is consistent with Liu et al. (2006). For AFs inside ICMEs, the total duration of AFs is 252.9 hr, about 12.6% of the total ICME duration (2011.5 hr) with the data gap removed. The occurrence rate of AFs inside

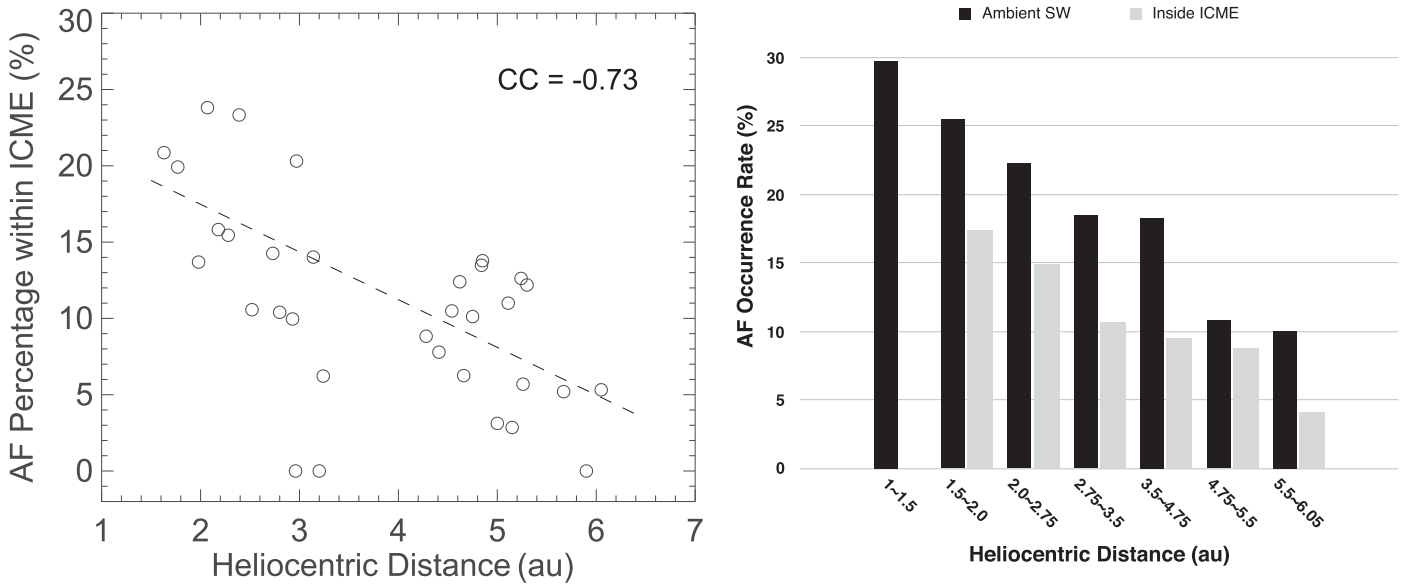

Figure 3. Left: dependence of the percentage of AF duration inside ICME on heliocentric distance. The dashed line denotes the linear fitting result. CC represents the correlation coefficient. Right: dependence of AF occurrence rate on heliocentric distance. The black bars represent occurrence rates in ambient solar wind, and the gray bars represent those inside ICMEs.

ICMEs decreases from about 17.3% at 1.5 ~ 2.0 to about 4.1% at 5.5 ~ 6.0 au. For AFs in ambient solar wind, the total duration of AFs is 1434.8 hr, about 16.4% of the total ICME duration (8756.4 hr) with the data gap removed. The occurrence rate of AFs in ambient solar wind decreases from about 29.8% at 1.0 ~ 1.5 to about 10.1% at 5.5 ~ 6.0 au.

To check the difference of the AF occurrence rates inside ICMEs and in ambient solar wind in terms of statistical significance, the Kolmogorov–Smirnov test is performed, suggesting that the AF occurrence rate in ambient solar wind is significantly different from that inside ICMEs with a probability of 96.3%.

5. INDIRECT EVIDENCE OF LOCAL ICME PLASMA HEATING BY AF DISSIPATION

By using the new approach of AF diagnosis, many intervals of AFs are identified inside ICMEs from 1 to 6 au. In addition, the percentage of AF duration inside ICME decreases generally linearly with heliocentric distance. Based on these two findings, we are more confident that AF dissipation inside ICMEs could contribute to local ICME plasma heating.

Here, we will show some indirect evidence to link local ICME plasma heating with AFs inside ICMEs. We divide each ICME duration into 10 segments and obtain the distribution of AF occurrence rate and normalized T_p/T_{ex} across ICMEs based on the superposed epoch analysis, as shown in Figure 4(a). The horizontal axis represents the relative location across the ICME cross-section. 0–10 denotes the lading edge of an ICME, 90–100 denotes the trailing edge of an ICME, and 40–60 denotes the center of an ICME. The green bars show the distribution of AF occurrence rate inside ICMEs, and the green line represents the polynomial fitting result. The blue bars give the distribution of normalized T_p/T_{ex}, and the blue line represents the polynomial fitting result. The distribution of AF occurrence rate inside ICMEs represents a clear "W" shape, indicating that the AFs are more frequently found in the center and at the boundaries of ICMEs. Similarly, the "W"-shaped distribution is obviously found in normalized T_p/T_{ex}, indicating

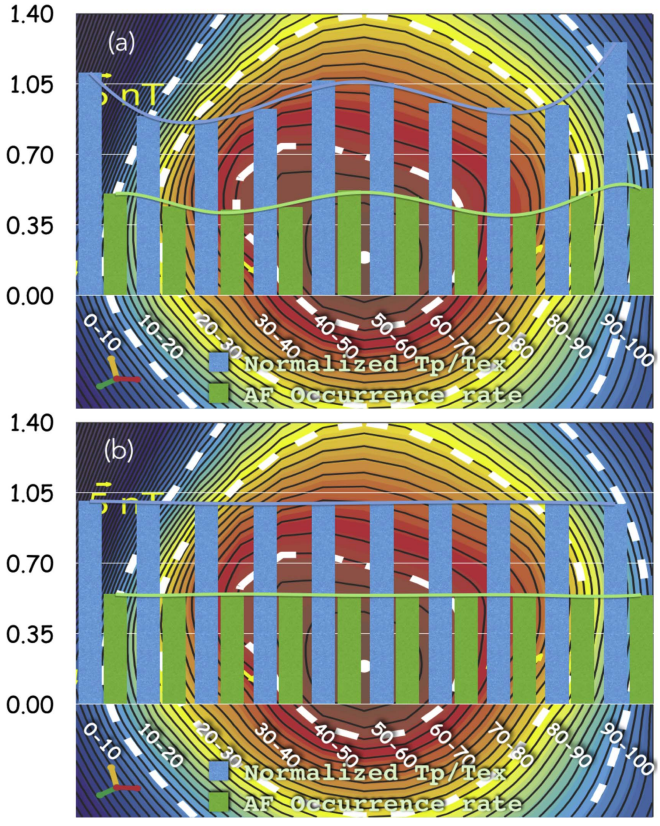

Figure 4. Distribution of AF occurrence rate and normalized T_p/T_{ex}: (a) across ICMEs based on the superposed epoch analysis; (b) in ambient solar wind based on the Monte Carlo test. Note that the AF occurrence rate has been multiplied by 1.5 and then increased by 0.3 to appear better together with normalized T_p/T_{ex}. The background figure, as adopted from Figure 9 in Hu & Sonnerup (2002), is used to illustrate the spacecraft trajectory through the magnetic cloud.

that the ICME plasma seems to be more heated in the center and at the boundaries of ICMEs. These findings suggest significant contribution of AFs on local plasma heating inside

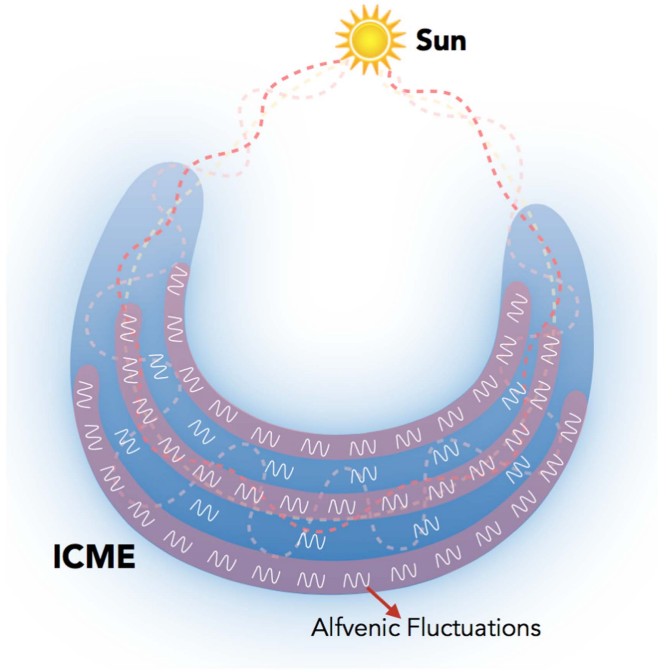

Figure 5. Sketch of ICME plasma heating due to AF dissipation. The white wave-like curve represents AF. Its spacing indicates the occurrence rate of AF inside ICMEs. The colors represent the plasma temperature. The light blue denotes cold, and the light red denotes warm.

ICMEs. In the literature, several mechanisms have been proposed to account for the plasma heating inside ICMEs. This work suggests a significant contribution of AF dissipation on local plasma heating inside ICMEs, but does not give a quantitative estimation of AF dissipation contribution, and neglects the contributions from other mechanisms. The other potential mechanisms may work together and contribute equally inside ICMEs.

For comparison, a Monte Carlo test is performed. We randomly select a control sample of 33 intervals in ambient solar wind with lengths similar to that of the ICMEs intervals and re-plot Figure 4(a) by 10,000 times. The results are shown in Figure 4(b). Similarly, the AF occurrence rate has been multiplied by 1.5 and then increased by 0.3 in order to appear better together with normalized T_p/T_{ex}. It is clear that both the "W"-shaped patterns of AF occurrence rate and normalized T_p/T_{ex} inside ICMEs are absent. The normalized T_p/T_{ex} and the AF distribution are both uniform during the whole interval. Nevertheless, the plasma heating by AF dissipation could also apply to the ambient solar wind outside ICMEs. Those results are due to randomly distributed AFs in the selected intervals and the effect of averaging.

To interpret these phenomena physically, some assumptions need to be made in advance. (1) The temperature inside ICMEs is nearly uniform at the beginning. (2) The whole ICME structure experiences the same expansion. (3) AFs inside ICMEs originate from the Sun's surface when the CME occurs. (4) AF distribution inside ICMEs is nonuniform. (5) The dissipation rates of AF inside ICMEs are identical. Figure 5 gives a sketch of ICME plasma heating due to AF dissipation. AFs are more frequently found in the center and at the boundaries of ICMEs. Considering a nearly identical dissipation rate, more AFs would be dissipated in the center and at the boundaries of ICMEs, after which more energy would contribute to ICME plasma heating in the center and at the boundaries. As ICMEs expand and propagate outward, the percentage of AF duration inside ICMEs keeps on decreasing with heliocentric distance, which has been confirmed in Section 4.

6. SUMMARY

Nonlinear cascade of low-frequency AFs is regarded as one of the major candidate mechanisms of local ICME plasma heating during its expansion and transportation. However, AFs inside ICMEs have been rarely reported in the literature. In this study, we identify 33 probable ICMEs observed by *Voyager* 2 between 1 and 6 au, finding that relatively pure AFs could be frequently seen inside 30 ICMEs with an average occurrence rate of 12.6%. Statistically, the percentage of AF duration inside ICMEs decays generally linearly as ICMEs expand and move outward. Compared to in ambient solar wind, the occurrence rate of AFs inside ICMEs is much less, especially within 4 au. Furthermore, the occurrence rate of AFs and the proton temperature inside ICMEs have similar "W"-shaped distributions, large in the center and at the boundaries of ICMEs. By assuming a uniform dissipation rate of AFs inside ICMEs, our findings provide indirect evidence of local ICME plasma heating due to AF dissipation.

We thank the *Voyager* Mission for the use of their data. The high-resolution *Voyager* 2 plasma data are publicly available at the *Voyager* Data Page of the Massachusetts Institute of Technology Space Plasma Group (ftp://space.mit.edu/pub/plasma/vgr/v2). The 48 s resolution magnetic field data are accessible at the NSSDC (ftp://nssdcftp.gsfc.nasa.gov). The authors would like to thank Dr. Shuo Yao for helpful discussions. This work was supported by 973 program 2012CB825602 and NNSFC grants 41574169, 41574168. H.L. was also supported by Youth Innovation Promotion Association of the Chinese Academy of Sciences and in part by the Specialized Research Fund for State Key Laboratories of China.

REFERENCES

Bemporad, A., Raymond, J., Poletto, G., & Romoli, M. 2007, ApJ, 655, 576
Burlaga, L. F. 1995, Interplanetary Magnetohydrodynamics (New York: Oxford Univ. Press)
Filippov, B., & Koutchmy, S. 2002, SoPh, 208, 283
Furth, H. P., Killeen, J., & Rosenbluth, M. N. 1963, PhFl, 6, 459
Galinsky, V. L., & Shevchenko, V. I. 2012, ApJ, 751, 146
Gopalswamy, N. 2010, in Proceedings of the 20th National Solar Physics Meeting, ed. I. Dorotovič (Hurbanovo: Slovak Central Observatory), 108
Gosling, J. T. 1990, in Physics of Magnetic Flux Ropes, ed. C. T. Russell, E. R. Priest, & L. C. Lee (Washington, DC: AGU), 343
Hu, Q., & Sonnerup, B. U. Ö 2002, JGR, 107, 1142
Kasper, J. C., Lazarus, A. J., & Gary, S. P. 2008, PhRvL, 101, 261103
Landi, E., Raymond, J. C., Miralles, M. P., & Hara, H. 2010, ApJ, 711, 75
Li, H., Wang, C., Belcher, J. W., He, J. S., & Richardson, J. D. 2016b, ApJL, 824, L2
Li, H., Wang, C., Chao, J. K., & Hsieh, W. C. 2016a, JGR, 121, 42
Liu, Y., Richardson, J. D., & Belcher, J. W. 2005, P&SS, 53, 3
Liu, Y., Richardson, J. D., Belcher, J. W., & Kasper, J. C. 2006, JGR, 111, A01102
Lopez, R. E. 1987, JGR, 92, 11189
Marsch, E., Yao, S., & Tu, C.-Y. 2009, AnGeo, 27, 869
Murphy, N. A., Raymond, J. C., & Korreck, K. E. 2011, ApJ, 735, 17
Neugebauer, M., & Goldstein, R. 1997, in Coronal Mass Ejections, ed. N. Crooker, J. A. Joselyn, & J. Feynman (Washington, DC: AGU), 245
Richardson, I. G., & Cane, H. V. 1995, JGR, 100, 23397
Richardson, J. D., Liu, Y., Wang, C., & Burlaga, L. F. 2006, AdSpR, 38, 528
Richardson, J. D., & Smith, C. W. 2003, GeoRL, 30, 1206
Russell, C. T., & Shinde, A. A. 2003, SSRv, 216, 285

Rust, D. M., & LaBonte, B. J. 2005, ApJL, 622, L69
Tam, S. W. Y., & Chang, T. 1999, GeoRL, 26, 3189
Tu, C.-Y., & Marsch, E. 1995, SSRv, 73, 1
Wang, C., Du, D., & Richardson, J. D. 2005, JGR, 110, A10107
Wang, C., & Richardson, J. D. 2004, JGR, 109, A06104
Wang, C. B., Wang, B., & Lee, L. C. 2014, SoPh, 289, 3895
Yao, S., Marsch, E., Tu, C.-Y., & Schwenn, R. 2010, JGR, 115, A05103
Zurbuchen, T. H., & Richardson, I. G. 2006, SSRv, 123, 31